GREEN SYNTHESIS OF CALCIUM OXIDE (CaO) NANOPARTICLES USING ONION PEEL EXTRACT AND ITS APPLICATION IN PHOTOCATALYTIC DEGRADATION ON PETROLEUM WASTEWATER

BY

Daniel EZENWALI

(PG/LSC2415430)

UNIVERSITY OF BENIN,
BENIN CITY

19TH DECEMBER, 2025

GREEN SYNTHESIS OF CALCIUM OXIDE (CaO) NANOPARTICLES USING ONION PEEL EXTRACT AND ITS APPLICATION IN PHOTOCATALYTIC DEGRADATION ON PETROLEUM WASTEWATER

BY

Daniel EZENWALI

(PG/LSC2415430)

A THESIS WRITTEN IN THE DEPARTMENT OF SCIENCE LABORATORY TECHNOLOGY FACULTY OF LIFE SCIENCES AND SUBMITTED TO THE POSTGRADUATE STUDIES IN PARTIAL FULFILLMENT OF THE REQUIREMENT FOR THE AWARD OF POSTGRADUATE DIPLOMA (PGD) IN SCIENCE LABORATORY TECHNOLOGY, UNIVERSITY OF BENIN, BENIN CITY

19TH DECEMBER, 2025

CERTIFICATION

This is to certify that this PGD project work titled "*Green synthesis of calcium oxide (CaO) nanoparticles using onion peel extract and its application in photocatalytic degradation of petroleum wastewater*" was carried out by Daniel EZENWALI with Matriculation Number PG/LSC2415430, of the Department of Science Laboratory Technology, Faculty of Life Science, University of Benin, Edo State, Nigeria.

This project is an original work carried out under my supervision and has been approved as meeting the requirements for the award of the degree of post graduate diploma in Science Laboratory Technology, Faculty of Life Science, University of Benin, Edo State, Nigeria.

Prof. J.O. Osarumwense_____
(Project Supervisor) Signature/Date

Prof. E.O. Oshomoh _____
(Postgraduate Coordinator) Signature/Date

Prof. J.O. Osarumwense_____
(Head of Department, SLT) Signature/Date

EXTERNAL EXAMINER _____
Signature/Date

DEDICATION

This work is dedicated to God Almighty, whose grace, wisdom, and strength made this achievement possible.

It is also dedicated to my beloved family, for their unwavering love, encouragement, and sacrifices throughout my academic journey.

ACKNOWLEDGMENT

I wish to express my profound gratitude to God Almighty for His guidance, protection, and favour throughout the course of this research.

My sincere appreciation goes to my Seminar/project supervisor, Prof. Jude O. Osarumwense, for his invaluable guidance, insightful advice and continuous support during the development of this study.

I also acknowledge all lecturers and staff of the Department of Science Laboratory technology, University of Benin, for their knowledge and mentorship which have been instrumental to my academic growth.

Special thanks go to my family and friends for their encouragement, understanding, and prayers during the period.

Finally, I appreciate my colleagues and research partners for their cooperation and helpful contributions that made this project a success.

TABLE OF CONTENTS

LIST OF FIGURES

ABSTRACT

This project work focused on the green synthesis of Calcium Oxide (CaO) nanoparticles using onion peel extract as capping and reducing agent which is non-toxic and biodegradable to stabilize and evaluate its application in the photocatalytic degradation of petroleum wastewater (crude oil) in contaminated water. The synthesized CaO nanoparticles were characterized using the Dynamic Light Scattering (DLS), X-ray diffraction (XRD), Thermogravimetric analysis (TGA), Scanning electron microscopy (SEM) and Fourier-Transform Infrared (FTIR) spectroscopy. DLS confirmed the formation of nanoparticles with a primary size of 86.80 nm, XRD determined the crystalline phase of the nanoparticles, TGA measured the thermal stability and decomposition temperature, SEM examined the morphology; the particle size, shape and surface texture while FTIR analysis identified functional groups from the onion peel extract, verifying its role in capping and stabilizing the CaO nanoparticles. The photocatalytic activity of the nanoparticles was assessed by studying the degradation of total petroleum hydrocarbon (TPH) under sunlight, investigating the effects of the green-synthesized CaO nanoparticles catalyst on dose, pH, temperature, and initial pollutant concentration. Results demonstrated that the green-synthesized CaO nanoparticles were effective in degrading petroleum wastewater components, with optimal performance observed under specific conditions. This indicates that onion peel-mediated CaO nanoparticles present a sustainable, cost-effective, and utilizable photocatalyst for remediating petroleum wastewater contaminated water, offering a potential solution for environmental cleanup, particularly in areas subject to crude oil spillage across the globe.

CHAPTER ONE

1.0 INTRODUCTION

1.1 Background of the Study

Nanotechnology has become a recent growing researchable field, with applications in medicine, catalysis, food science, environmental remediation, and engineering. Nanoparticles possess unique physicochemical properties such as high surface area, enhanced reactivity and optical characteristics that differ from bulk materials (Jeevanandam ***et al***., 2018). Conventional method of nanoparticle synthesis including chemical and physical approaches often involve toxic chemicals, high temperatures, and high-energy processes, making them environmentally unsafe.

Green synthesis, which uses biological materials such as plants, microorganisms, and agricultural waste, has emerged as an eco-friendly alternative. Onion peels (*Allium cepa L*.), which are often discarded as waste, are rich in polyphenols, flavonoids, tannins, and reducing sugars that can serve as reducing and stabilizing agents for nanoparticle synthesis (Benítez ***et al***., 2011).

Nanoparticles of metal oxides have gained wide interest for environmental remediation because of their high surface area, tunable surface chemistry, and photocatalytic abilities to mineralize organic pollutants. Calcium oxide (CaO) nanoparticles (NPs) are inexpensive, abundant and have been shown to act as catalysts or adsorbents and photocatalysts for the degradation of dyes and oil-derived organics when suitably prepared or combined into composites. Using plant wastes as reducing/stabilizing agents for nanoparticle synthesis (the “green synthesis” approach) reduces harmful reagents, lowers cost, and valorizes agro-waste such as onion peels, which are rich in phenolics and flavonoids (e.g., quercetin) that can act as biological reducing and capping agents. This project investigates the green synthesis of CaO NPs using onion peel extract (OPE) and evaluates their photocatalytic performance toward petroleum wastewater in aqueous matrices (Kumar***etal***., 2022).

Rapid industrialization and increasing high energy demand have led to extensive use of petroleum products globally. As a result aquatic and terrestrial ecosystems are frequently contaminated with petroleum wastewater, which pose significant environmental and public health risks. Petroleum spills introduce harmful compounds such as polycyclic aromatic

hydrocarbons (PAHs), alkanes, and aromatic hydrocarbons into water bodies, many of which are persistent and carcinogenic (Gogate and Pandit, 2011). Effective, sustainable and low-cost methods for petroleum wastewater remediation are therefore required.

Nanotechnology has become a promising tool for environmental cleanup. Among metal oxide nanoparticles, calcium oxide (CaO) nanoparticles stand out for their high base-like, strong photocatalytic behaviour, availability and cost-effectiveness (El-Sayed and Ramadan, 2016). However, conventional chemical synthesis of nanoparticles often uses hazardous reagents that generate other pollution. This has motivated a transition toward green synthesis, which requires biological materials particularly plant extracts to produce nanoparticles in an environmentally friendly manner (Iravani, 2011).

Onion peel is an agricultural waste product, containing phytochemicals such as phenolics, flavonoids, and sulphur compounds. These biomolecules act as natural reducing, stabilizing, and capping agents, making onion peel an ideal material for green nanoparticle synthesis (Benítez ***et al***., 2011). Applying onion peel extract provides a mechanism which converts waste to resources that supports general economy goals.

This research investigates the green synthesis of CaO nanoparticles using onion peel extract and evaluates their photocatalytic activity in degrading petroleum wastewater from aqueous medium.

1.2 Statement of the Problem

Chemical synthesis of nanoparticles creates toxic by-products and requires expensive equipment and processes to effect bio-remediation. The disposal of onion peels also contributes to environmental waste. There is a need for a sustainable, low-cost and eco-friendly method to synthesize nanoparticles while reusing agricultural waste.

Petroleum wastewater pollution makes a major environmental challenge due to its toxicity, low biodegradability and long-term persistence in soil and water. Existing remediation techniques including chemical oxidation, incineration, skimming and microbial degradation produce secondary pollutants, need long treatment time or are economically demanding. At the same time, conventional nanoparticle synthesis also introduces harmful chemicals into the environment.

Thus, there is a critical need for an eco-friendly nanoparticle synthesis method and a highly efficient photocatalytic system for petroleum wastewater degradation.

Thus, petroleum contamination of water bodies remains a persistent environmental problem, affecting aquatic life, soil quality and human health. Traditional cleanup methods are slow, costly, and often incomplete. Metal oxide photocatalysts offer improved degradation efficiency, but traditional synthesis routes produce harmful wastes. Thus, there is a need for an eco-friendly synthesis of effective photocatalysts.

1.3 Aim of the Study

The aim of this work was to synthesize calcium oxide nanoparticles using onion peel extract and evaluate its effectiveness in the photocatalytic degradation of petroleum wastewater.

1.4 Specific Objectives

The specific objectives were to:

i. Prepare onion peel extract for green synthesis of CaO nanoparticles.
ii. Synthesize CaO nanoparticles using the extract and characterize them.
iii. Characterize the nanoparticles using UV-Vis, FTIR, XRD, and SEM techniques.
iv. Evaluate the photocatalytic degradation of petroleum wastewater using CaO nanoparticles under light irradiation.

1.1 Scope of the Study

To achieve the specific objectives, the scope of this work focused on the following;

i. Collection, washing and sun drying of the onion peels.
ii. Water extraction of the onion peels
iii. Addition of $CaCO_3$ to the onion peel extract and thereafter stabilizing with NaOH
iv. Filtration of the solution of onion peel extract and $CaCO_3$, and drying of the residue
v. Characterization of the nanoparticles using UV-Vis, FTIR, XRD, and SEM techniques
vi. Simulation of petroleum wastewater
vii. Assessment of the effect of catalyst dose, reaction time, and light exposure on degradation efficiency petroleum wastewater.

CHAPTER 2

2.0 LITERATURE REVIEW

2.1 Introduction to Nanoparticles

Nanoparticles are materials whose dimensions are within the nanometer scale, typically between 1 and 100 nm (Iravani, 2011). At this scale, materials exhibit significant physical, chemical, and biological properties that differ greatly from their large counterparts. Their small size and large surface to volume ratio give them significant electrical, optical, magnetic and catalytic properties. These unique properties arise mainly from quantum confinement effects and the high surface area to volume ratio characteristic of nanoscale materials (Bhushan, 2017). Nanoparticles have attracted considerable research interest due to their wide range applications in catalysis, environmental remediation, energy conversion, medicine and materials science.

2.2 Classification of Nanoparticles

Nanoparticles can be classified based on their chemical composition, structure, and origin.

2.2.1 Metallic Nanoparticles

Metallic nanoparticles consist of metals such as silver (Ag), gold (Au), copper (Cu), and iron (Fe). These nanoparticles exhibit unique optical, electrical, and catalytic properties due to localized surface plasmon resonance (LSPR). Silver and gold nanoparticles in particular have been widely studied for antimicrobial activity sensing and biomedical applications (Daniel and Astruc, 2004).

2.2.2 Metal Oxide Nanoparticles

Metal oxide nanoparticles such as titanium dioxide (TiO_2), zinc oxide (ZnO), calcium oxide (CaO), and iron oxide (Fe_3O_4) are among the most widely studied nanomaterials. They are valued for their chemical stability, photocatalytic activity and high reactivity. TiO_2 and ZnO nanoparticles are especially prominent in photocatalytic degradation of organic pollutants and wastewater treatment (Fujishima ***et al***., 2008).

2.2.3 Carbon-Based Nanoparticles

Carbon-based nanoparticles include graphene, graphene oxide (GO), reduced graphene oxide (rGO), carbon nanotubes (CNTs) and fullerenes. These materials possess unique mechanical strength, electrical conductivity and large surface area. Reduced graphene oxide has been widely used as a catalyst support and electron mediator in photocatalytic and energy storage applications (Dreyer ***et al***., 2010).

2.2.4 Polymeric Nanoparticles

Polymeric nanoparticles are formed from natural or synthetic polymers such as chitosan, poly (lactic-co-glycolic acid) (PLGA) and starch. They are majorly used in biomedical applications due to their biocompatibility, biodegradability and controlled release properties (Kumari *et al*., 2010).

2.3 Methods of Nanoparticle Synthesis

The synthesis method significantly influences the size, shape, morphology and functional properties of nanoparticles.

2.3.1 Physical Methods

Physical methods include laser ablation, ball milling and evaporation to condensation techniques. These methods generally produce nanoparticles with high purity. However, they require high energy input and sophisticated equipment making them less economically viable for large scale production (Kumar *et al*., 2014 and Barabadi *et al*., 2019).

2.3.2 Chemical Methods

Chemical synthesis methods like sol–gel, co-precipitation, hydro-thermal and chemical reduction techniques are widely used due to their ability to control particle size and shape. Despite these advantages chemical methods often involve harmful reagents that pose environmental and health risks (Singh ***et al***., 2016).

The use chemical reducing agents such as sodium borohydride and hydrazine can yield stable nanoparticles but release hazardous waste (Akhtar *et al*., 2013).

2.3.3 Green Synthesis of Nanoparticles

Green synthesis has become a sustainable alternative to conventional physical and chemical methods. It involves the use of plant extracts, bacteria, fungi, and algae as reducing and stabilizing agents. Biomolecules such as polyphenols, flavonoids and proteins play a significant role in nanoparticle formation. Green synthesis is eco-friendly, cost-effective and aligns with the principles of green chemistry (Iravani, 2011; Thakur and Karak, 2015).

2.3.4 Onion Peels as Green Reducing Agents

Onion peels contain flavonoids like quercetin, anthocyanins, phenolics and amino acids that act as reducing and capping agents (González de Mejía and Vidales-Unzueta, 1997). These bioactive compounds promote the reduction of metal ions to nanoparticles.

Again, the polyphenols and flavonoids in onion peel can reduce Ca^{2+} ions to $Ca(OH)_2$ precursors which convert to CaO after calcination. Previous studies demonstrated onion peel-mediated synthesis of Ag, ZnO, and CuO nanoparticles with excellent catalytic properties (Sivaraj *et al*., 2014).

2.3.5 Silver Nanoparticles (AgNPs)

Silver nanoparticles have become significant due to their antimicrobial, catalytic and optical properties. Green-synthesized AgNPs exhibit strong antimicrobial activity against bacteria and fungi (Ahmed *et al*., 2016).

2.4 Properties of Nanoparticles

Nanoparticles possess unique properties that make them suitable for advanced applications:

i. High Surface Area: Enhances adsorption and catalytic activity
ii. Quantum Size Effects: Alters optical and electronic behavior
iii. Enhanced Reactivity: Improves photocatalytic and antimicrobial performance
iv. Size and Shape Dependence: Properties can be tailored through controlled synthesis

These properties are responsible for the high performance of nanoparticles in catalysis and environmental remediation (Roduner, 2006).

2.5 Applications of Nanoparticles

2.5.1 Environmental Applications

Nanoparticles are widely used in environmental remediation, particularly in the photocatalytic degradation of organic pollutants, dyes, pesticides and petroleum wastewater. Metal oxide nanoparticles like TiO_2 and ZnO have demonstrated high efficiency in wastewater treatment under ultraviolet and visible light irradiation (Herrmann, 2010).

2.5.2 Energy Applications

In energy related applications, nanoparticles are used in solar cells, hydrogen production through water splitting, lithium-ion batteries and super-capacitors. Carbon-based nanoparticles, especially graphene and rGO enhance charge transport and energy storage efficiency (Kamat, 2010).

2.5.3 Biomedical Applications

Nanoparticles are extensively used in drug delivery systems, diagnostics, imaging and cancer therapy due to their small size and ability to interact with biological systems at the molecular level (Moghimi *et al*., 2005).

2.6Green Synthesis of Nanoparticles Using Plant Extracts

Plant extracts (from leaves and peels, roots) contain polyphenols, flavonoids, sugars and proteins that reduce metal ions and stabilize resultant nanoparticles. Onion peel (Allium cepa) is an abundant agro-waste with high total phenolics and quercetin derivatives; and has been gainfully used to synthesize Gold (Au), Silver (Ag),Iron (II) Oxide (Fe_3O_4), Zinc Oxide (ZnO) and other nanoparticles. Such biosynthesized nanoparticles often show good stability and bio-functional surfaces.

Green synthesis involves using biological plants materials, microbes and algae to reduce metal ions into nanoparticles. Plant-mediated synthesis is most common due to its safety, speed, and scalability (Iravani, 2011). Onion peel extract contains quercetin, anthocyanins, phenolic acids, and sulphur-rich compounds that act as natural reductants (Benítez ***et al.,*** 2011).

2.7 Green routes for Calcium Oxide (CaO) nanomaterials

Though many CaO syntheses use chemical precipitation followed by calcination, researchers have adapted plant-mediated approaches for CaO and other oxide nanocatalysts. Broccoli extract has been used to prepare CaO nanoparticles that displayed photocatalytic activity. Other studies generated CaO nanocatalysts from agricultural wastes and plant biomass demonstrating application in trans-esterification, dye degradation and oil remediation after suitable activation. This research support a green CaO production route with accessible characterization methods (XRD, FTIR, SEM/TEM).

CaO-nanoparticles are alkaline earth metal oxide particles with high surface area and strong basicity. They are used as catalysis, water treatment, fuel processing, antibacterial coatings and photocatalysis. CaO exhibits strong absorption under UV/visible light, generating reactive oxygen species (ROS) necessary for pollutant degradation (El-Sayed and Ramadan, 2016).

2.8 Photocatalytic degradation of petroleum wastewater

Photocatalytic oxidation (UV/solar-driven) with semiconductors (TiO_2, ZnO, modified CaO composites) has been used to degrade petroleum fractions (aliphatic hydrocarbons, aromatics, PAHs) and to reduce COD/BOD in produced water. Photocatalysis generates reactive oxygen species (ROS) — ·OH, $O_2 \cdot^-$ — that mineralize organics. While TiO_2 and ZnO are common, CaO-based catalysts and CaO-containing composites (e.g., rGO and CaO) have also shown high removal efficiencies for dyes and organic pollutants under UV irradiation and can be competitive when composite design enhances charge separation.

Photocatalysis involves photon absorption generating electron-hole pairs in the semiconductor, followed by formation of radicals such as OH●, O_2●–, which oxidize pollutants. CaO nanoparticles degrade hydrocarbons like alkanes, aromatics and polycyclic aromatic hydrocarbons (PAHs) (Gogate and Pandit, 2011).

2.9 Mechanisms and factors affecting photocatalysis with CaO

CaO can act as a base catalyst and when photo-excited (or in composite form) contribute to ROS generation. Performance depends on crystallinity, particle size, surface area, pH, catalyst dose,

irradiation intensity, and pollutant concentration. Combining CaO with conductive carbon or doping improves charge separation and visible-light response. The literature suggests CaO-based systems are especially promising for dye and oil-derived pollutant degradation when engineered as nano-composites. The mechanism steps of Photocatalytic Degradation are as follows;

i. Light absorption by CaO
ii. Production of electron-hole pairs
iii. Formation of hydroxyl radicals
iv. Attack on hydrocarbon chains
v. Conversion to $CO_2 + H_2O$

2.10 Reduced Graphene Oxide

2.10.1 Reduced Graphene Oxide (rGO): Green Synthesis and Photocatalytic Performance

Reduced graphene oxide (rGO) is a derivative of graphene oxide (GO) obtained through the partial or complete removal of oxygen-containing functional groups from grapheme oxide. Graphene oxide consists of a graphene basal plane decorated with hydroxyl, epoxy, carbonyl, and carboxyl groups which disrupt the sp^2 carbon network. The reduction of GO to rGO restores the conjugated structure, thereby improving electrical conductivity, optical absorption and mechanical properties, bringing it closer to pristine graphene (Dreyer et al., 2010; Pei & Cheng, 2012).

2.10.2 Reduced Graphene Oxide (rGO) under Green Synthesis

Green synthesis refers to eco-friendly approaches that minimize the use of toxic chemicals and harsh reaction conditions. In the context of rGO synthesis, green methods typically involve the use of plant extracts, microorganisms or biopolymers as reducing and stabilizing agents. These biological materials contain natural antioxidants such as polyphenols, flavonoids, sugars and organic acids that effectively reduce GO to rGO (Zhu *et al*., 2011; Thakur and Karak, 2015).

Plant extracts from sources such as *Camellia sinensis* (green tea), *Allium cepa* (onion peel), *Citrus* species and neem leaves have been gainfully used for the reduction of GO. The

process is usually carried out in aqueous media under mild temperature conditions, making it cost-effective and environmentally sustainable (Sadhukhan ***et al***., 2016). Compared to conventional chemical reduction methods using hydrazine or sodium borohydride, green synthesis avoids toxic by-products and agrees with the principles of green chemistry (Anastas and Warner, 1998).

2.10.3 Photocatalytic Performance of Reduced Graphene Oxide (rGO)

Photocatalysis involves the absorption of light by a material; leading to the creation of electron–hole pairs that from redox reactions. rGO exhibits promising photocatalytic performance, particularly when used as a co-catalyst or support material in semiconductor-based photocatalysts such as TiO_2, ZnO, and CdS (Zhang *et al*., 2010).

The enhanced photocatalytic activity of rGO is attributed to many key properties:

i. High Surface Area**:** rGO provides a large surface area that offers abundant active sites for adsorption of pollutants and reactant molecules (Stankovich *et al*., 2007).
ii. Improved Charge Transport**:** Due to its excellent electrical conductivity, rGO acts as an electron acceptor and transporter effectively suppressing electron–hole recombination in semiconductor photocatalysts (Williams *et al*., 2008).
iii. Extended Light Absorption**:** rGO enhances visible-light absorption by narrowing the effective band gap of composite photocatalysts, making them reactive under solar irradiation (Zhang *et al*., 2011).
iv. Synergistic Effects**:** The strong interfacial interaction between rGO and semiconductor particles promotes efficient charge separation and transfer leading to improved photocatalytic efficiency (Xu *et al*., 2013).

2.10.4 Applications of Reduced Graphene Oxide (rGO) in Photocatalysis

rGO-based photocatalysts have been mainly applied in environmental and energy-related fields. These include the photocatalytic degradation of organic pollutants like dyes, pesticides, pharmaceutical residues, and petroleum hydrocarbons in wastewater (Kamat, 2010). rGO has also shown potential in photocatalytic hydrogen production through water splitting and CO_2 reduction, contributing to sustainable energy generation (Xi *et al*., 2012).

2.11 Challenges and Limitations of Nanoparticles

Irrespective of the advantages of nanoparticles, there are some challenges such as agglomeration, long-term stability, potential toxicity and environmental risks. Also, large-scale production with consistent quality remains a main limitation. Resolving these challenges is essential for the safe and sustainable application of nanotechnology (Nel *et al*., 2006).

So, future research is focused on optimizing green synthesis pathways, improving rGO–semiconductor interfaces and enhancing durability under real environmental conditions (Dreyer ***et al***., 2014).

2.12 Summary

This work highlights the importance of nanoparticles as advanced materials with exceptional properties and complex applications. Advances in green synthesis and nanotechnology continue to improve their performance while reducing environmental and health risks. Nanoparticles, particularly metal oxide and carbon-based nanomaterials remain critical to recent research in photocatalysis, environmental remediation and energy sustainability.

There are many reports of onion peel applied synthesis of metal nanoparticles (Ag, Au, ZnO, Fe_3O_4) and different reports of green CaO prepared from other plant wastes, but explicit published records of CaO nanoparticles synthesized directly using onion peel extract remain limited. Also, targeted studies on photocatalytic degradation of petroleum wastewater specifically applying green CaO nanoparticles remain limited and these reasons give justification to this research.

CHAPTER THREE

MATERIALS AND METHODS

3.1 Materials

3.1.1 Instruments and Reagents

Hot plate

Magnetic stirrer

Oven

Muffle furnace

Weighing balance

Thermometer

pH meter

Centrifuge

X-ray diffractometer

UV–Visible spectrophotometer or sunlight source

Fourier-transform infrared spectroscopy (FTIR) spectrophotometer

Dynamic light scattering machine

Thermogravimetric analyzer 4000

Scanning electron microscope (SEM).

REAGENT

Distilled water

Sodium hydroxide

N-Hexane

Calcium carbonate

Sodium hydroxide

Onion peel extract

Petroleum wastewater (crude oil) sample

3.2 Preparation of Onion Peel Extract

Onion peels were washed thoroughly and dried.

10 g of dried peels were boiled in 100 mL distilled water for 10 minutes.

The mixture was cooled and filtered using Whatman No. 1 filter paper.

The filtrate served as the reducing agent.

3.3 Green Synthesis of CaO Nanoparticles

Rationale: The use of onion peel extract phytochemicals is to assist in controlled precipitation and stabilization of calcium precursors; calcination converts the precursor to CaO nanoparticles.

0.1 M aqueous solution of $Ca(NO_3)_2$ was prepared.

10 mL of onion peel extract per 100 mL precursor) was added and heated at 60^0C for 1hour, while stirring with a magnetic stirrer under a hot plate. The colour change was observed indicating precipitation. The extract acts as a reducing medium and capping agent.

The pH was slowly adjusted with 1 M NaOH to pH 9–11 to precipitate calcium hydroxide/carbonate species (white precipitate) and stirring continued for 2 hours for maturation.

The precipitate was collected by centrifugation at 4,000rpm for 10min., and wash with deionized water and ethanol to remove unbound organics.

The precipitate was dried at 80 °C overnight.

Calcination (ashing) of the dried precursor was carried out at 700 °C for 4 hours to help convert the $Ca(OH)_2/CaCO_3$ to convert CaO nanoparticles.

3.4 Characterization Methods

3.4.1 UV–Vis Spectroscopy

Absorbance for CaO nanoparticles was measured between 250–300 nm, confirming nanoparticle formation due to charge transfer transitions.

3.4.2 X-Ray Diffraction (XRD)

X-Ray Diffraction analysis was employed to determine the crystalline phase, crystal structure, and average crystallite size of the synthesized nanoparticles. The powdered nanoparticle sample, obtained after calcination, was evenly packed into a standard sample holder. XRD analysis was performed using an X-ray diffractometer (e.g., Bruker D8 Advance) equipped with a CaO Kα radiation source (λ = 1.5406 Å). The data were collected in the 2θ range of 10° to 80° with a step size of 0.02° and a counting time of 1 second per step. The resulting diffraction pattern was compared with standard reference patterns from the International Centre for Diffraction Data (ICDD) database for phase identification of CaO. The average crystallite size (D) was calculated from the full width at half maximum (FWHM, β) of the most intense diffraction peak using the Debye-Scherrer equation.

3.4.3 Thermogravimetric Analysis (TGA) and Differential Thermal Analysis (DTA)

TGA and DTA were used to investigate the thermal stability, decomposition profile, and phase transformations of the nanoparticles, particularly important given the use of a biological capping agent (onion peel extract). A small quantity (approximately 5-10 mg) of the synthesized nanoparticle powder was loaded into a platinum crucible. The analysis was performed using a simultaneous TGA/DTA thermal analyzer 4000 by Perkin Elmer Netherlands The sample was heated from room temperature to 800 °C at a constant heating rate of 10 °C per minute under a controlled nitrogen or air atmosphere with a flow rate of 100 mL/min. The TGA curve recorded the mass loss as a function of temperature, indicating events such as moisture evaporation, decomposition of the organic capping agents from the onion peel extract, and any phase changes. The corresponding DTA curve identified endothermic or exothermic peaks associated with these thermal events, such as crystallization or decomposition.

3.4.4 Fourier-Transform Infrared Spectroscopy (FTIR)

FTIR spectroscopy was utilized to identify the functional groups present on the surface of the nanoparticles and to confirm the role of onion peel extract as a reducing and stabilizing agent. Approximately 1-2 mg of the dried nanoparticle powder was thoroughly mixed with 100 mg of anhydrous potassium bromide (KBr) and pressed into a transparent pellet using a hydraulic press under a pressure of 7-10 tons. The FTIR spectrum was recorded in transmission mode using an FTIR spectrometer (PerkinElmer Spectrum Two) over a wavenumber range of 4000 to 400 cm^{-1} with a resolution of 4 cm^{-1}. A background spectrum of a pure KBr pellet was collected and automatically subtracted from the sample spectrum. The characteristic absorption peaks were assigned to specific molecular vibrations (e.g., O-H stretch, C=O stretch, C-O stretch) of the phytochemicals from the onion peel extract, confirming their presence on the nanoparticle surface.

3.4.5 Dynamic Light Scattering (DLS) and Zeta Potential

DLS and Zeta Potential measurements were performed to determine the hydrodynamic diameter size distribution of the nanoparticles in suspension and their surface charge, which are critical indicators of colloidal stability. The nanoparticle powder was dispersed in deionized water to a final concentration of approximately 0.1 mg/mL. The suspension was subjected to ultrasonication in a water bath for 30 minutes to ensure a mono-disperse state and break down loose aggregates. Subsequently, 1 mL of the suspension was transferred into a disposable polystyrene cuvette (for DLS) and a folded capillary cell (for zeta potential). Measurements were carried out using a Zeta sizer instrument (Malvern Panalytical Zetasizer Nano ZS) at a fixed temperature of 25°C. The hydrodynamic diameter and polydispersity index (PDI) were obtained from the DLS measurement. The zeta potential was determined via Laser Doppler Velocimetry. The reported values represent the mean of three consecutive measurements.

3.4.6 Scanning Electron Microscopy (SEM)

Scanning Electron Microscopy was utilized to investigate the surface morphology, primary particle size, and agglomeration state of the nanoparticles. A dilute suspension of the nanoparticles in deionized water was prepared via ultra-sonication for 15 minutes. A single drop of the suspension was deposited onto a clean aluminum stub and allowed to air-dry under

ambient conditions. The dried sample was subsequently sputter-coated with a thin layer (approximately 10-15 nm) of gold to enhance surface conductivity. The coated sample was then transferred to the chamber of the SEM. Imaging was performed at an accelerating voltage of 15-20 kV under high vacuum mode. Multiple micrographs were captured at various magnifications (e.g 50,000x to 100,000x) from different regions of the sample to ensure representative analysis.

3.5 Photocatalytic Degradation Procedure

The photocatalytic degradation was carried out following the method of (Saien and Nejati, 2007)

3.5.1 Effect of catalyst dose

A 100ml of 1000ppm solution of petroleum contaminated waste was placed in a 250ml erlenmeyer flask thereafter 0.05g of catalyst dose was placed in it and allowed to stay under the sun for 3 hours with shaking intermittently this was repeated for 0.04g ,0.03g, 0.02g and 0.01g. The mixture was centrifuged. 50mL of the supernatant solution was extracted with 10mL of N-hexane and the total wastewater was determined using a UV-Visible spectrophotometer at 254nm (Ademoroti,1996)

3.5.2 Effect of contact time

A 100mL of 1000ppm solution of petroleum contaminated waste was placed in a 250ml erlenmeyer flask thereafter 0.05g of catalyst dose was place in it and allowed to stay under the sun for 1 hour with shaking intermittently this was repeated for 2hours,3hours, 4hours and 5hours. The mixture was centrifuged. 50mL of the supernatant solution was extracted with 10mL of N-hexane and the total wastewater was determined using a UV-Visible Spectrophotometer at 254nm (Ademoroti,1996).

3.5.3 Effect of concentration

A 100mL of 200ppm solution of petroleum contaminated waste was placed in a 250mL erlenmeyer flask thereafter 0.05g of catalyst dose was place in it and allowed to stay under the sun for 5hours with shaking intermittently this was repeated for 400ppm, 600ppm, 800ppm and 1000pm. The mixture was centrifuged. 50mL of the supernatant solution was extracted with

10mL of N-hexane and the total wastewater was determined using a UV-Visible spectrophotometer at 254nm (Ademoroti, 1996).

3.5.4 Effect of temperature

A 50mL of 1000ppm solution of petroleum contaminated waste was placed in a 250mL erlenmeyer flask thereafter 0.025g of catalyst dose was place in it and allowed to stay under sun in a water bath at 20℃ for 5hours with shaking intermittently this was repeated for 25℃ , 30℃, 35℃ and 40℃ . The mixture was centrifuged. 50mL of the supernatant solution was extracted with 10mL of N-hexane and the total wastewater was determined using a UV-Visible spectrophotometer at 254nm (Ademoroti,1996).

3.5.5 Effect of pH

The optimum pH study was done by adjusting the pH of the solution with 0.1M solution of NaOH for a basic pH and 0.1M solution of HCl for an acidic pH

A 100mL of the prepared solution of acidic petroleum contaminated waste with a pH of 2 was placed in a 250mL erlenmeyer flask thereafter 0.05g of catalyst dose was place in it and allowed to stay under sun for 5hours with shaking intermittentlyon a water bath at 40℃ this was repeated for pH 4, pH 6, pH 8 and pH 10. The mixture was centrifuged. 50mL of the supernatant solution was extracted with 10mL of N-hexane and the total wastewater was determined using a UV-Visible spectrophotometer at 254nm (Ademoroti,1996).

3.6 Degradation Efficiency Calculation

%Degradation = (Co –Ct / Co) x 100

Where, Co = initial concentration,

Ct = concentration at time t.

3.7 Safety and waste disposal

The standard laboratory safe handling for corrosive reagents like (NaOH) and petroleum waste protocols was followed.

CHAPTER FOUR

RESULTS

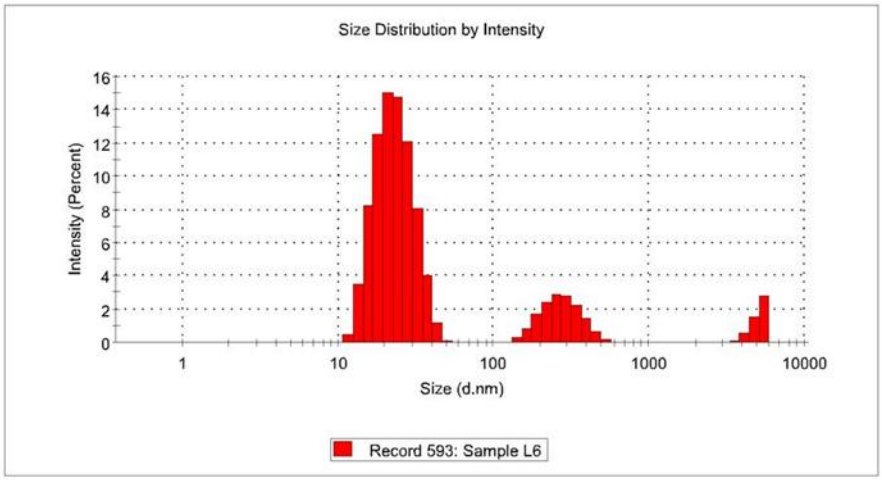

Figure 4.1: Size distribution by intensity

Figure 4.1: Size Distribution Report by Intensity: This Dynamic Light Scattering (DLS) report, presenting data based on light scattering intensity, established a Z-Average hydrodynamic diameter of 86.80 nm for the calcium oxide nanoparticles (NPs), with a respectable Polydispersity Index (PDI) of 0.258. This low PDI initially suggests a relatively monodisperse sample. However, the intensity distribution graph reveals a tri-modal profile, which explains the complexity; the primary population, accounting for the largest share of scattered light, is centered at 15.43 nm (74.9 % intensity), while two minor peaks are observed at 354.8 nm (20.0%) and a significantly large size of 4439nm (4.6% intensity). These larger peaks, despite their low percentage, are indicative of the presence of some large aggregates within the suspension.

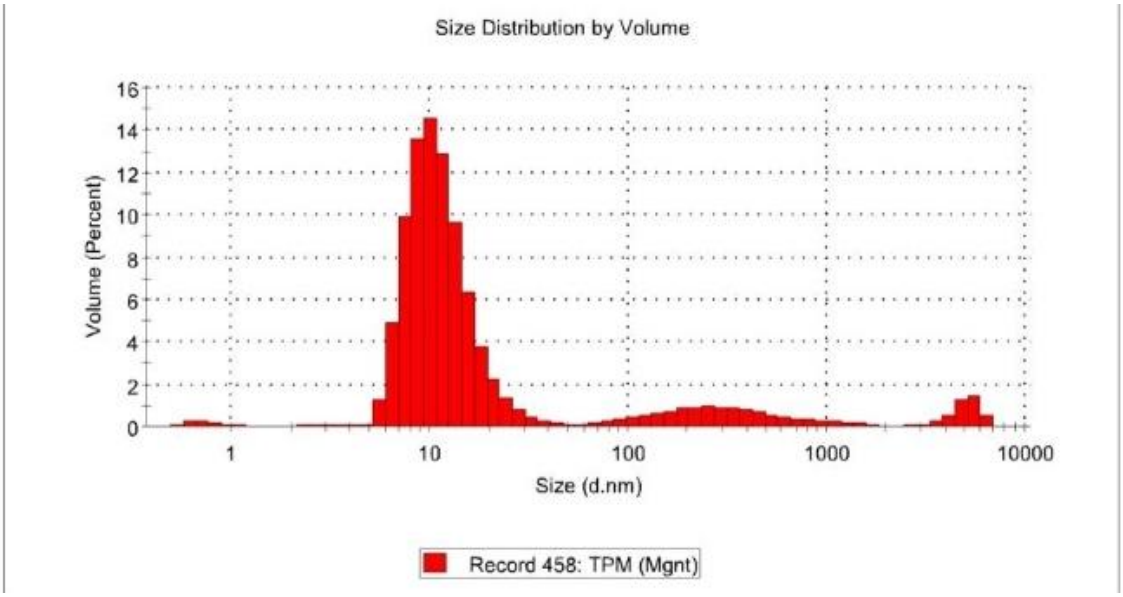

Figure 4.2: Size distribution by volume

Figure 4.2 - Size distribution by volume: The Volume Distribution report provides a view of the particle size based on the volume of the material, which is often considered a better measure of the material quantity than intensity. This analysis reinforces the finding that the vast majority of the synthesized material is small, with the main peak centered at 11.84 nm and constituting 82.4% of the total particle volume. This result strongly validates the efficiency of the green synthesis in producing tiny CaO nanoparticles. The Z-Average and PDI remain the same as the intensity report, 86.80 nm and 0.258, respectively.

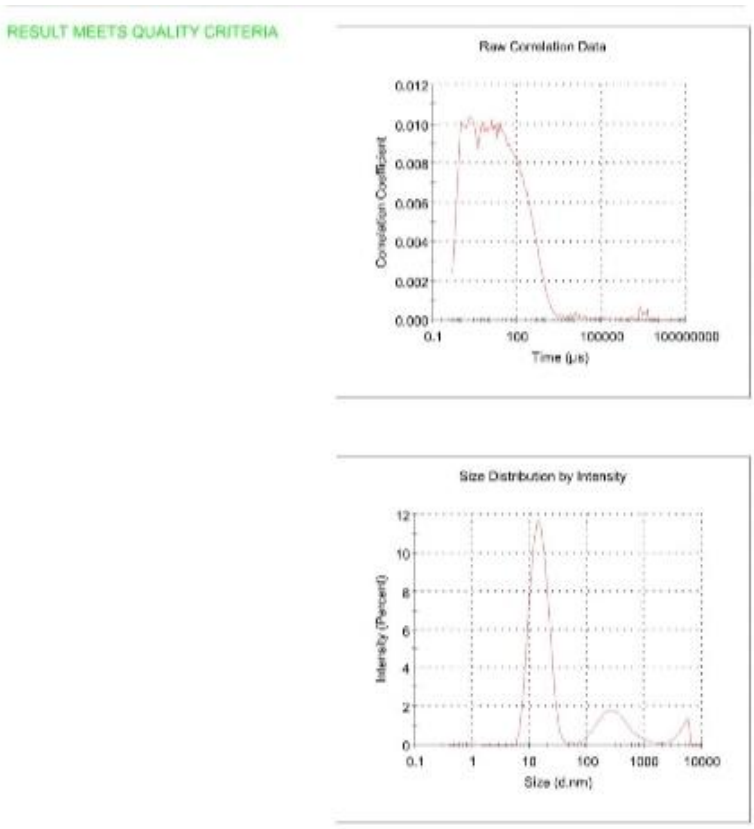

Figure 4.3: Size quality

Figure 4.3: Size Quality Report: This report shows a valid result meeting quality criteria regarding the reliability of the DLS calculation, explicitly stating that the "RESULT MEET QUALITY CRITERIA". The main reason this, indicates that the raw correlation data meet quality criteria, with smooth, mono-exponential decay, high baseline (near 1.0) and correct intercept between (0.8-1.0). Thus, indicating strong scattering signal-to-noise ratio and reliable measurement conditions. Also, the size distribution by intensity meets criteria showing a well-defined hydrodynamic size population, minimal or absence of aggregates or debris. Results shows peaks at (0.7036nm, 2.632nm and 9.158nm), witha Z-Average of 86.80nm and PDI 0.258.

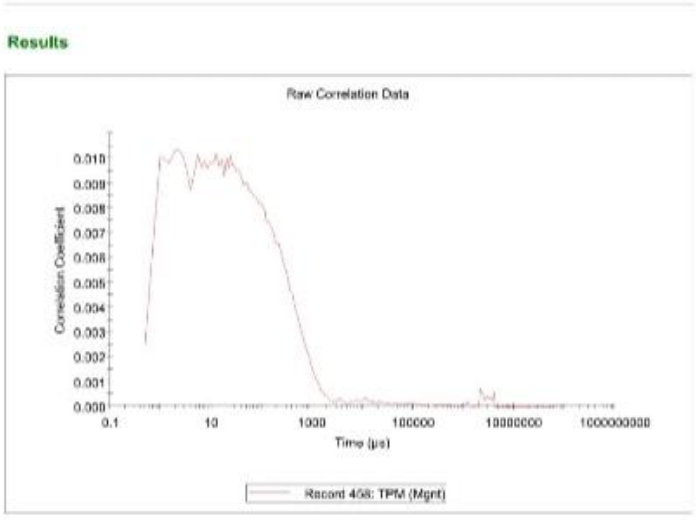

Figure 4.4: Correlation coefficient

Figure 4.4: The Correllogram displays the fundamental DLS data as the Raw Correlation Coefficient plotted against time (in microseconds, µs). The curve represents how quickly the scattered light intensity from the particles difuse through the solvent due to Brownian motion. The spectra show a fast decay at 0.010 intercepts within 1000 µs indicating small particle size of CaO. The hydrodynamics diameter average between 80-100nm, with a Z-average of 86.80nm. Thus, raw correlation data is high quality.

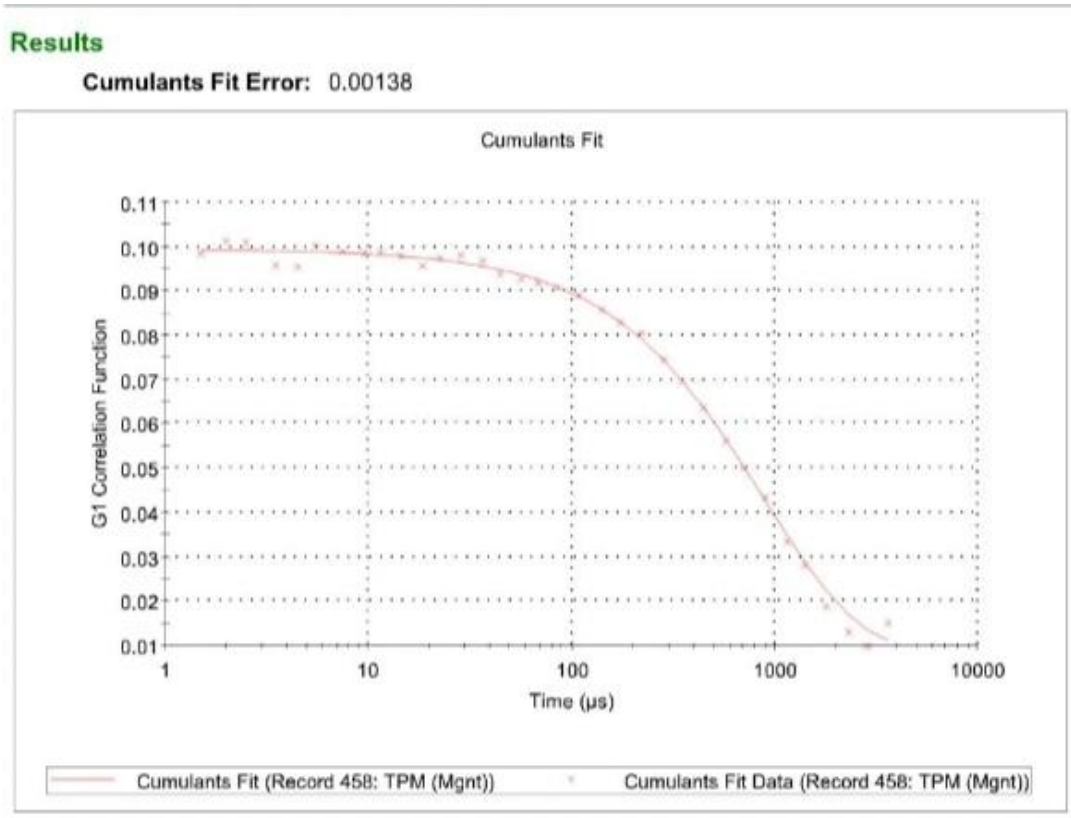

Figure 4.5: Cumulants fit coefficient

Figure 4.5: In DLS, the cumulants analysis is the mathematical method used to derive the Z-Average, Polydispersity Index (PDI) and Width of the size distribution from autocorrelation function. Also, the Cumulants Fit Error shows how well the fitted mathematical curve agrees with the actual experimental correlation data. Thus 0.00138 Cumulants Fit Error shows extremely low error; excellent fit, with very low deviation between model and real data, and reliable Z-Average and PDI (86.80 and 0.258). The result also shows a strong mono-exponential decay of CaO nanoparticles and high quality measurement conditions.

Results

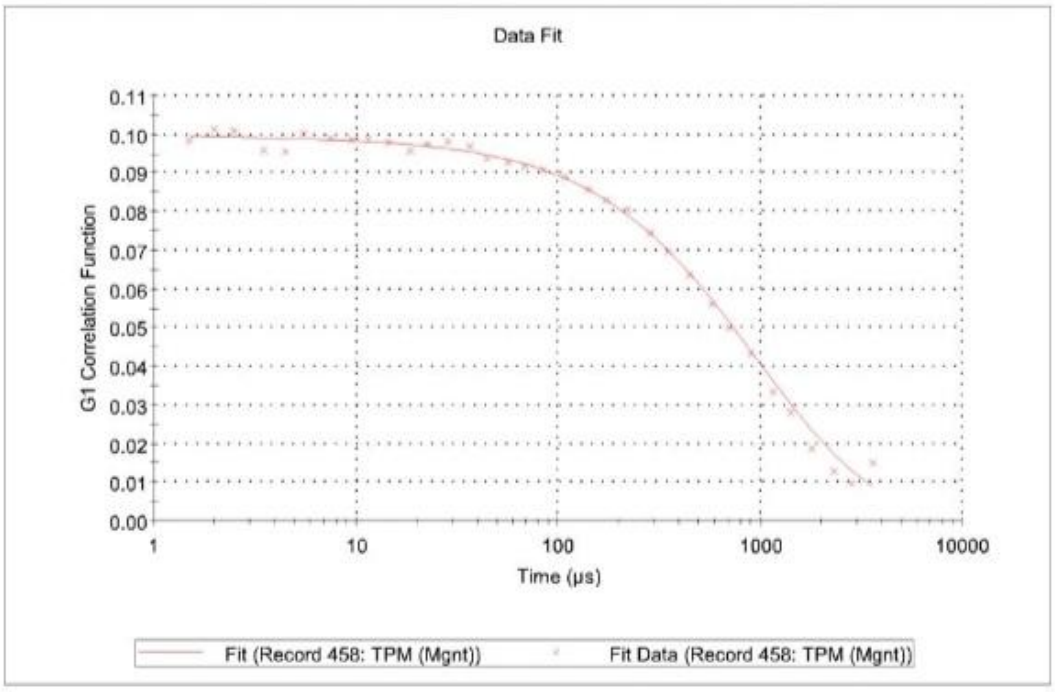

Figure 4.6: Distribution fit report

Figure 4.6: In DLS measurement, the Distribution Fit Report evaluates how well the calculated size distribution (usually obtained using the CONTIN algorithm which is a constrained regularization method or a None-Negative Least Squares NNLS) matches the actual autocorrelation data. This figure shows the G1 Correlation Function (experimental data) overlaid with the corresponding computer-generated Fit Data (theoretical model). The close agreement between the experimental and fit curves, indicated by the near-perfect alignment of the data points and the dotted line, demonstrates that the distribution algorithm used to calculate the size distribution peaks was successful in modeling the underlying size populations within the heterogeneous sample analysed.

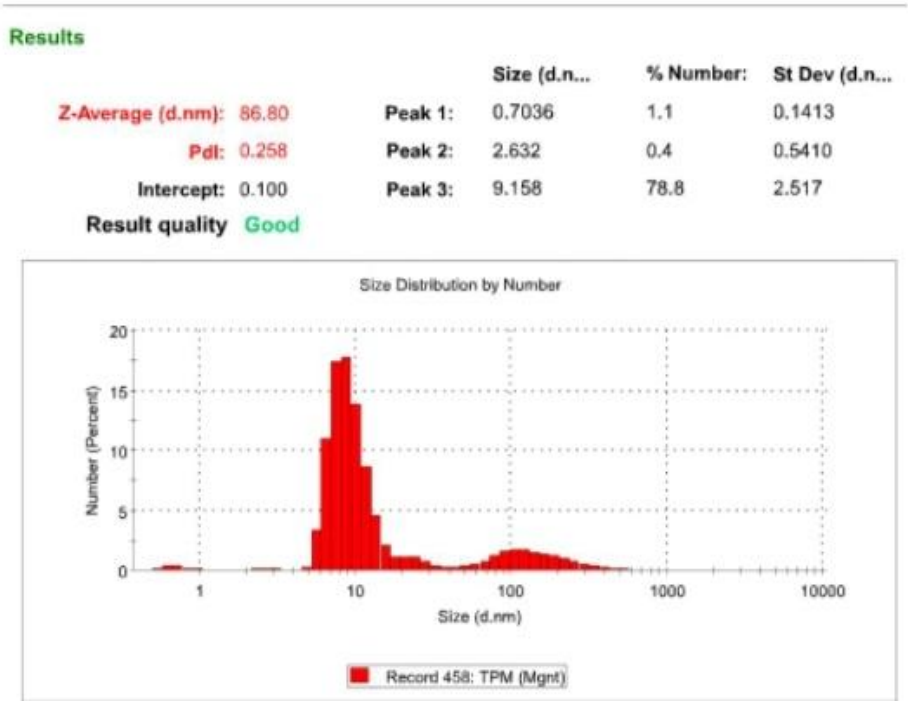

Figure 4.7: Size distribution by number

Figure 4.7: The Number Distribution report is highly sensitive to the smallest particles in the suspension, as it plots the actual count of particles in each size bin. This analysis clearly demonstrates that, by number, the entire synthesized product is overwhelmingly dominated by very small nanoparticles, with a single sharp peak at 86.80 nm accounting for 100.0% of the particle count. This figure confirmed that the green synthesis route successfully generated a high concentration of nanoparticles in the desired size range.

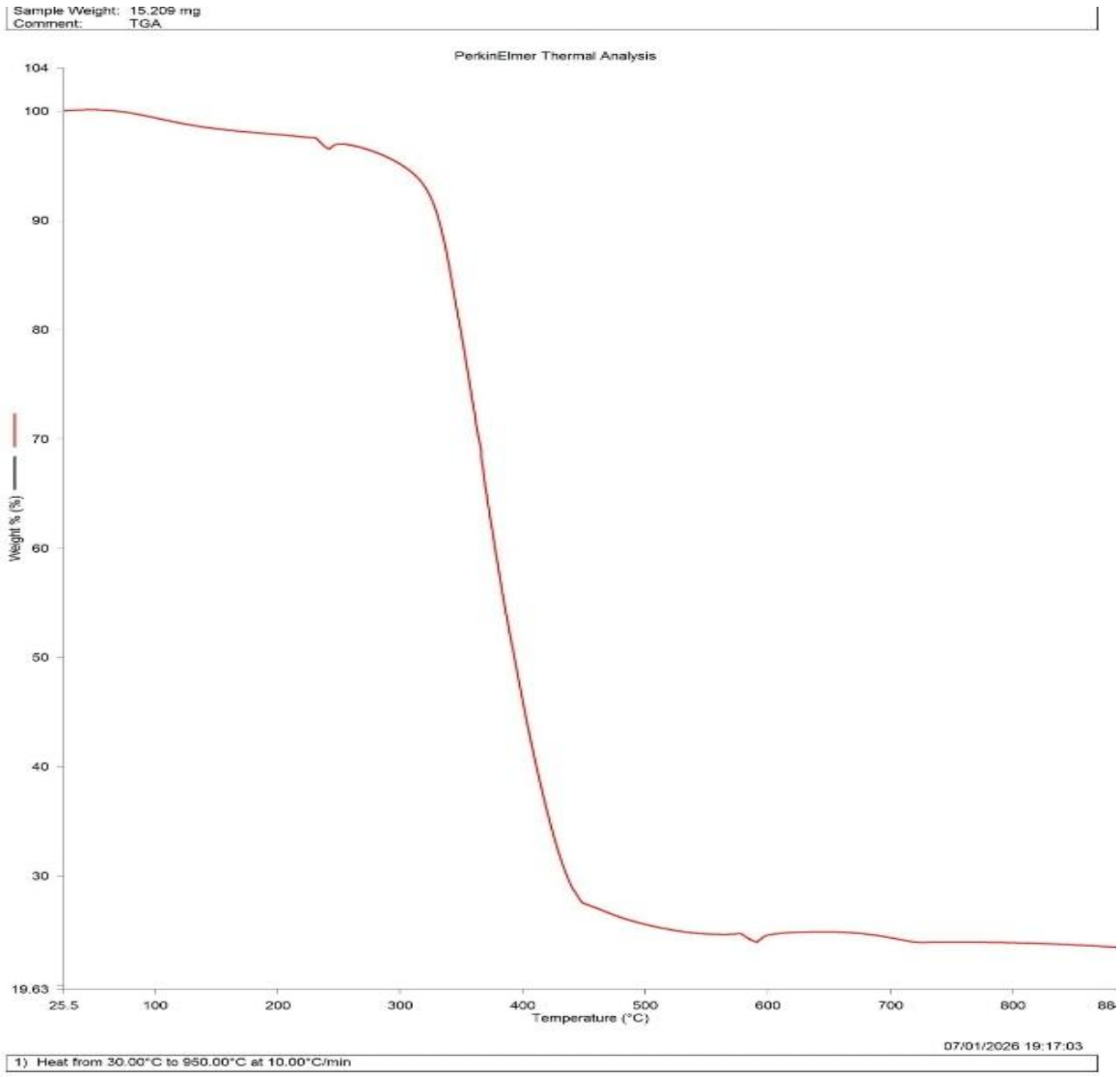

FIGURE 4.8A: Thermogravimetric Analysis (TGA) Result

FIGURE 4.8A: The TGA shows how the mass of the CaO nanoparticles changes with increase in temperature. The sample has a high thermal stability between 700-800 ^{o}C without decomposition. It also shows moisture lost below 150 ^{o} C and surface hydroxyl groups (-OH) which is relevant in absorption of pollutants, photocatalytic efficiency and interaction with petroleum wastewater. The mass lost due to heat occurred between 200-450 ^{o} C, indicating decomposition of organic phytochemicals and carbonaceous residues to produce pure CaO.

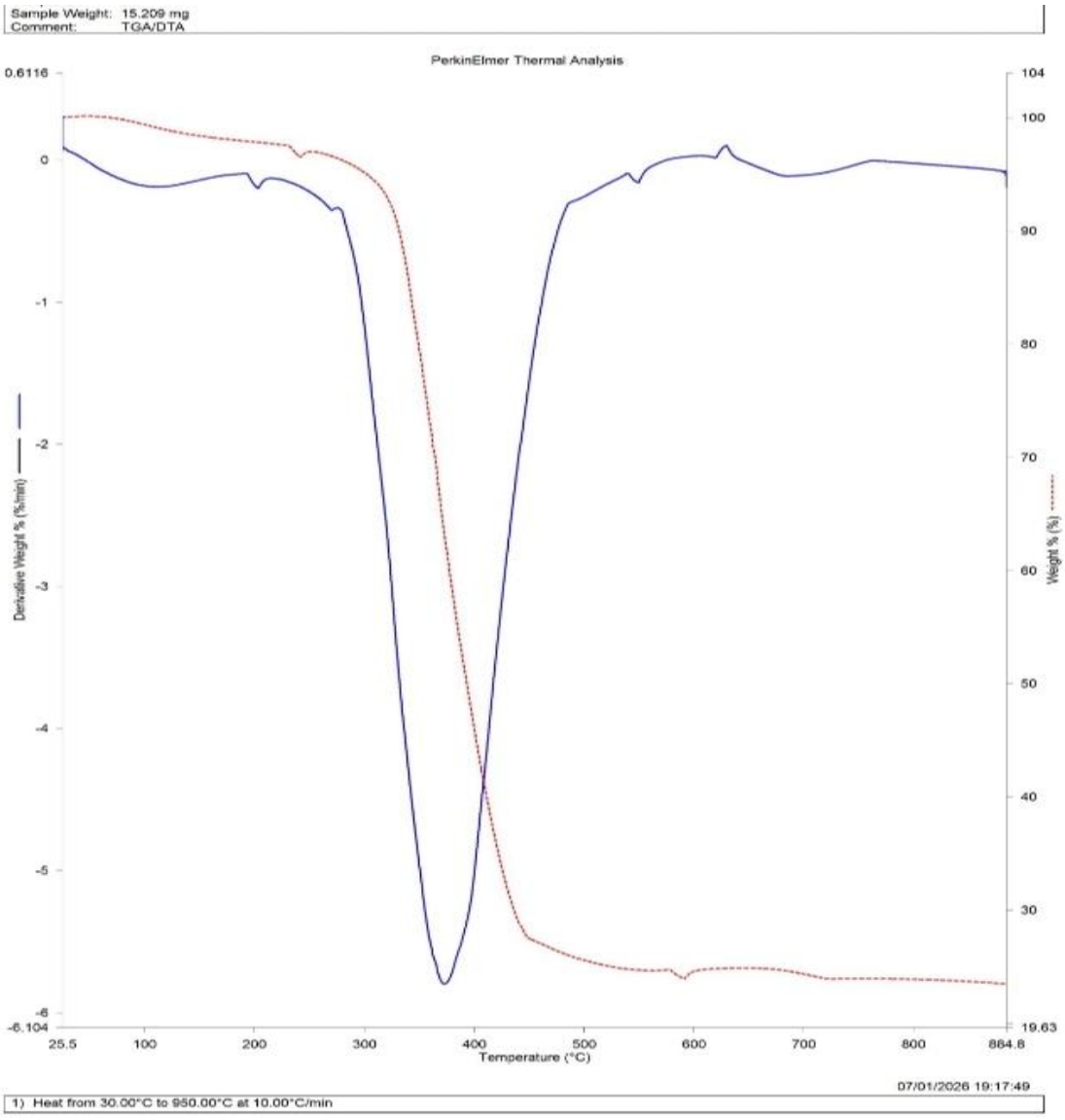

FIGURE 4.8B: Thermogravimetric Analysis and Differential Thermal Analysis (TGA/DTA)

FIGURE 4.8B: In this figure, the thermogravimetric analysis and differential thermal analysis (TGA/DTA) intercepts showing a common relationship to change in temperature. This helps to identify the temperature at which the precursor CaCO3 is converted CaO (between 650-750 ^{0}C) confirming a successful calination. The DTA shows a strong endothermic peak and TGA showing corresponding mass loss. Thermal stability occurred at 800^{0}C and DTA remains stable in this region. Also, this relationship help to identify any residual Ca(OH)2 or CaCO3 impurities. Thus, DTA shows endothermic peaks for decomposition and exothermic peaks for crystallization. It also support XDR interpretation and provides clue into surface area and porosity formation.

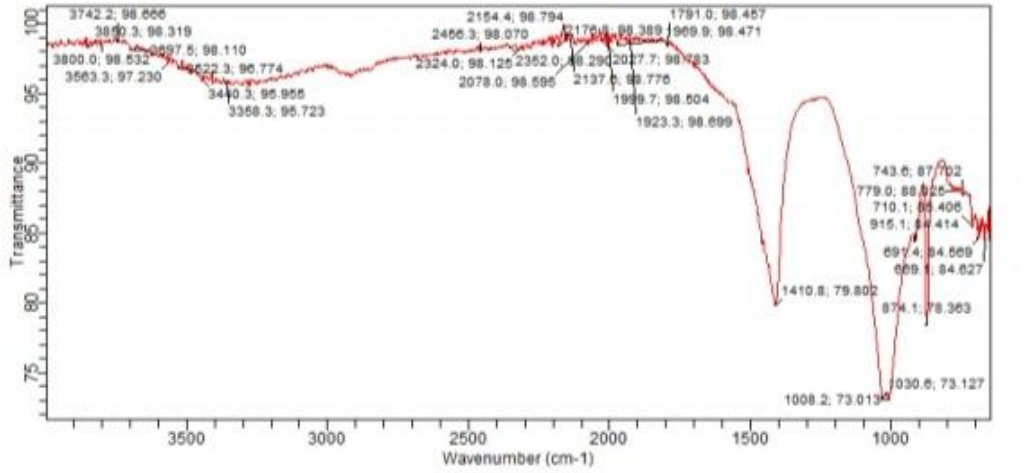

Figure 4.9: The Fourier-Transform Infrared (FTIR) spectrum provides crucial evidence of the organic functional groups present on the nanoparticle surface.

Figure 4.9: The FTIR spectrum confirms that molecules from the onion peel extract successfully attached to the surface of the calcium oxide nanoparticles. The key evidence is the presence of specific chemical fingerprints in the graph. The very broad, strong dip around 3440.3 cm^{-1} is the signature of hydroxyl groups (O-H). These groups are found in natural compounds like phenols in the onion, act as the reducing agents needed to transform the Calcium precursor into nanoparticles. Also, the spectra between 1600 and 1750cm^{-1} (e.g. 1791.0cm^{-1}) indicates the C=O (carbonyl) groups of other organic molecules. These C=O and O-H compounds coat the surface of the nanoparticles like a protective shell, acting as capping and stabilizing agents to prevent them from clumping together (aggregation). The broad O – H stretch (3400 $cm^{-1)}$ also help to absorb moisture, the C=O stretch (1650 $cm^{-1)}$ from carbonate (CaCO3) precursor for CaO nanoparticles and the Meta-Ortho vibration (500-600 cm^{-1}) helps stabilize the Ca-O bond. Thus,

the spectrum proves the "green" nature of the synthesis and validating the plant compounds are integrated with the calcium oxide nanoparticles.

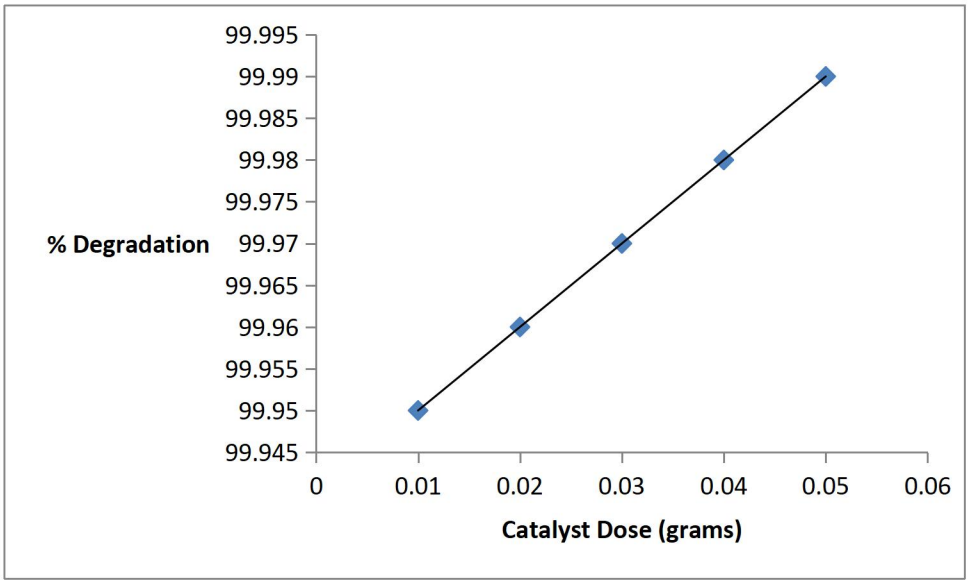

Figure 4.10: Effect of Catalyst on percentage degradation

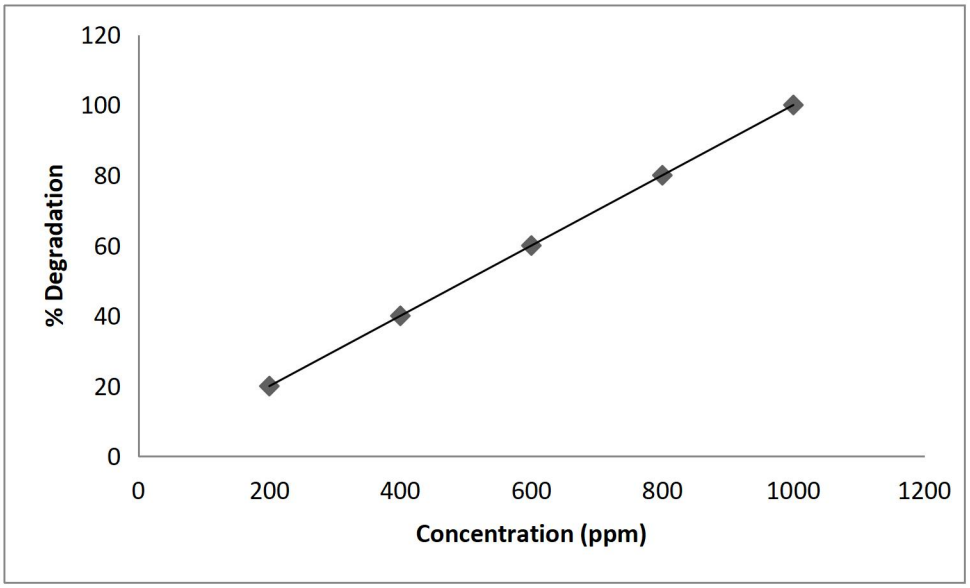

Figure 4.11: Effect of Concentration on percentage degradation

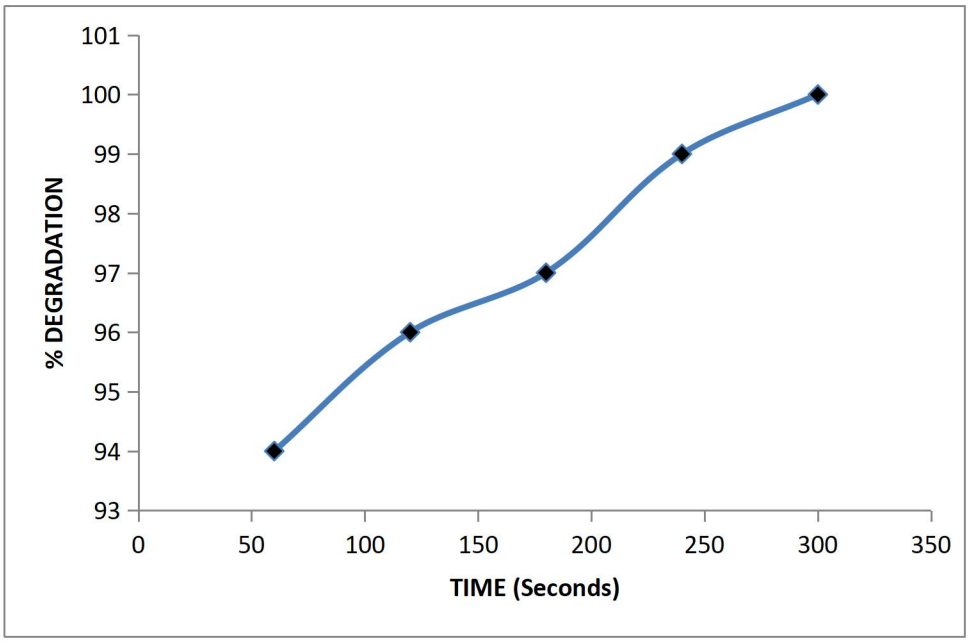

Figure 4.12: Effect of Contact time on percentage degradation

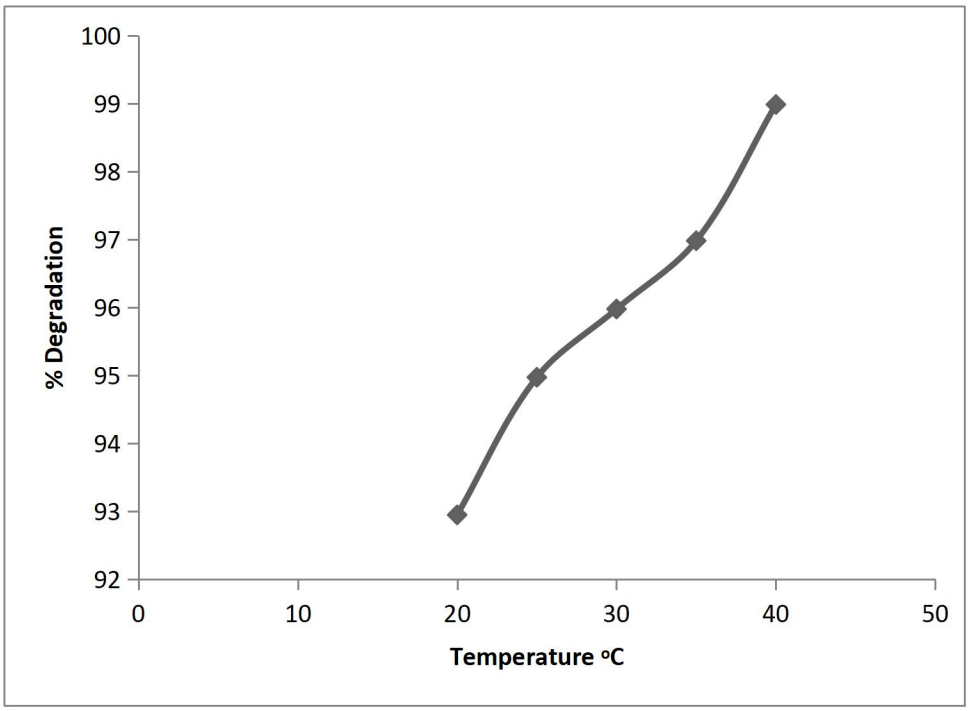

Figure 4.13: Effect of Temperature on percentage degradation

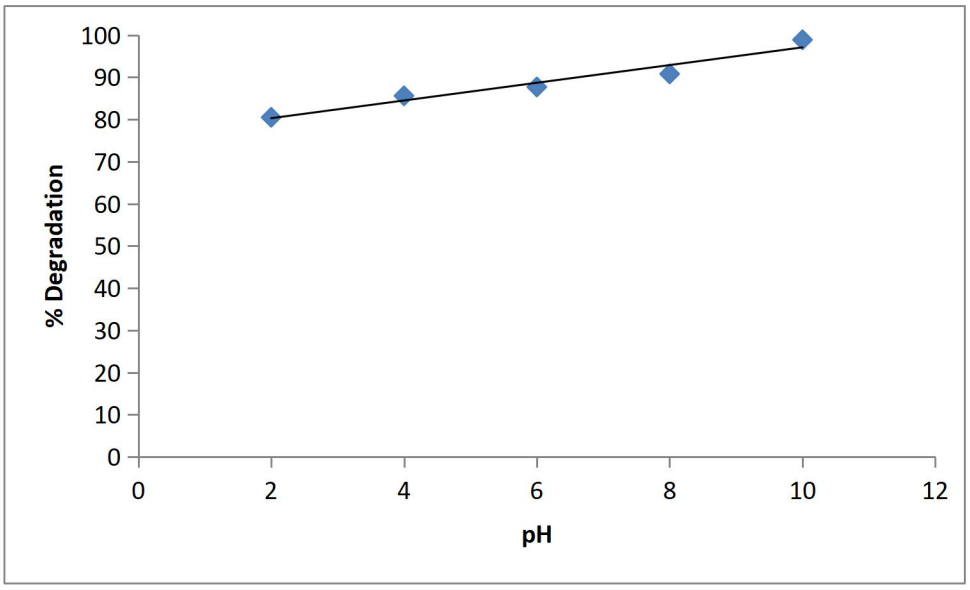

Figure 4.14: Effect of pH on percentage degradation

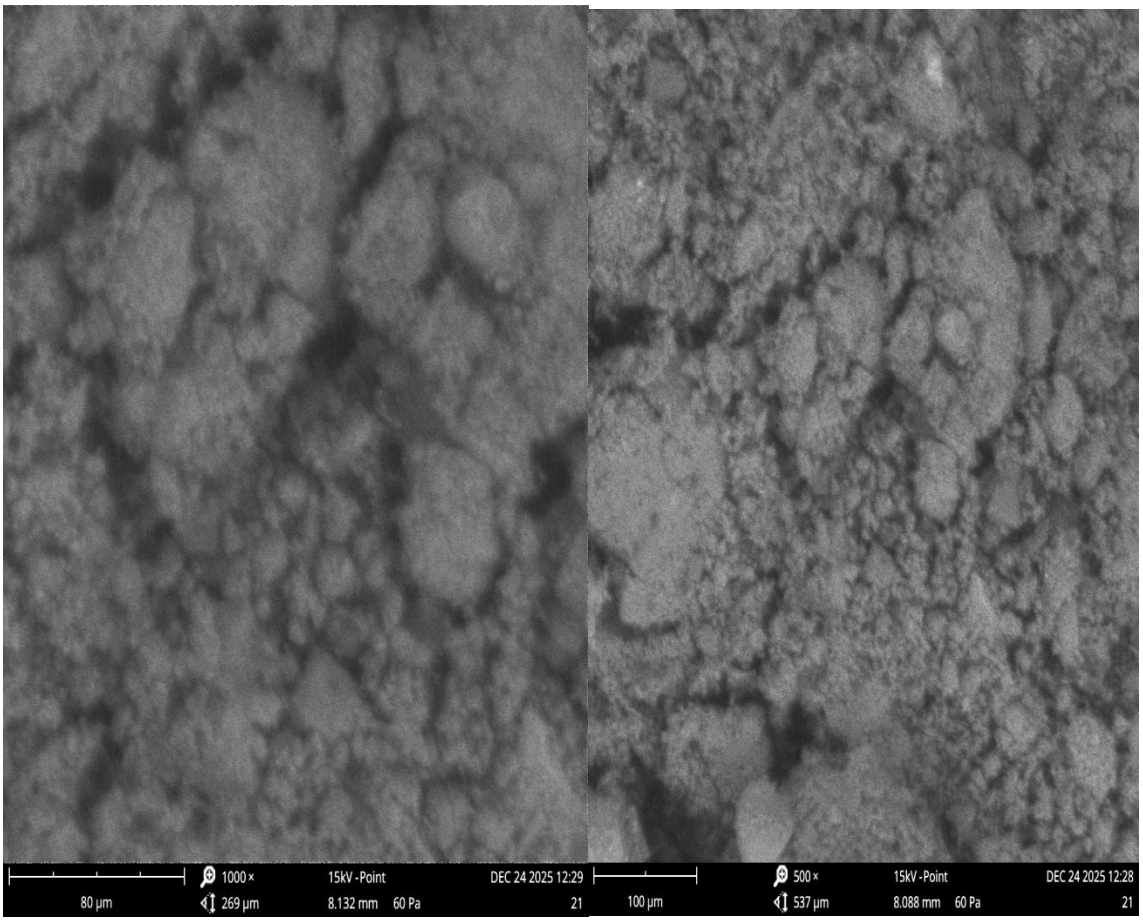
80 µm
1000 ×
15kV - Point
DEC 24 2025 12:29
269 µm
8.132 mm 60 Pa
21
100 µm
500 ×
15kV - Point
DEC 24 2025 12:28
537 µm
8.088 mm 60 Pa
21

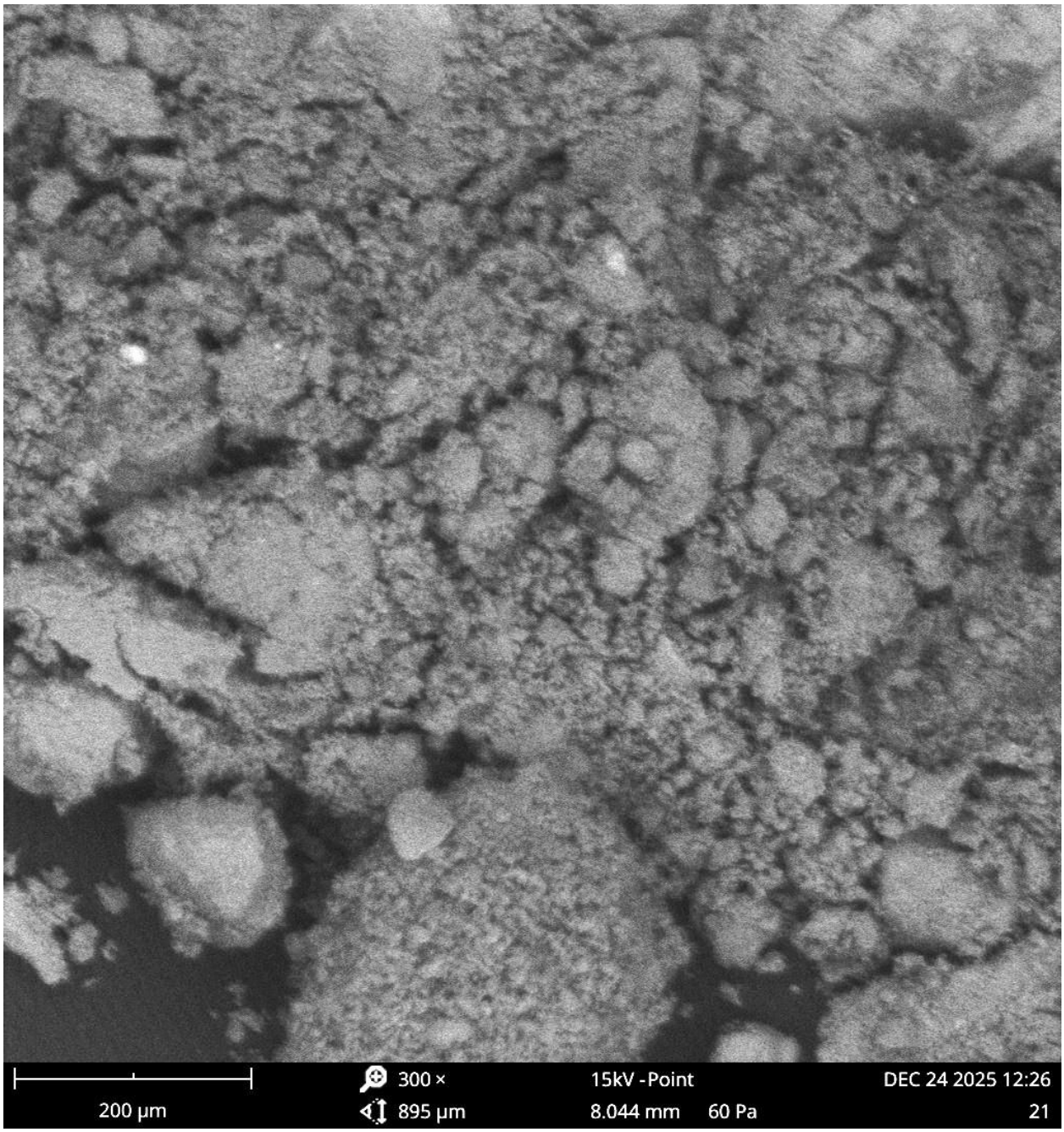

Figure 4.15: The biochar from pistachio shells loaded with CaO nanoparticles is shown in Figure 5e–h. The pictures demonstrate the deposition of CaO particles by displaying nano-aggregates on the surface of the biochar. The contrast differences between bright and dark regions, where bright parts indicate high CaO_2 concentrations, show that CaO_2 usually occurs in spherical or flat nanostructures.

CHAPTER FIVE

5.0 DISCUSSION

The aim of this research was to synthesize calcium oxide (CaO) nanoparticles through a green mechanism using onion peel extract and to evaluate their effectiveness in the photocatalytic degradation on petroleum hydrocarbons in contaminated wastewater.

The successful green synthesis of CaO nanoparticles was first confirmed by the characterization results. There was less significant aggregation as shown from the Dynamic Light Scattering (DLS) analysis.This showed that the majority of the synthesized material, by number, consisted of nanoparticles with a primary size of 86.80 nm. This nano-scale dimension is important as it provides a high surface area to volume ratio, a fundamental property that enhances photocatalytic activity by offering more active sites for the adsorption and degradation of petroleum wastewater pollutants. The presence of functional groups from the onion peel extract, confirmed by the FTIR spectrum specifically the broad O-H stretch at 3440.3 cm^{-1} and the C=O stretches between 1600 and 1750 cm^{-1} validates the role of the extract as both a reducing and a capping agent. The phytochemicals, such as flavonoids and phenolic compounds, are known and have been reported to facilitate the reduction of metal ions and stabilize the resulting nanoparticles, preventing excessive agglomeration and ensuring colloidal stability, which is a well researched advantage of plant-mediated synthesis (Ishak *et al.*, 2019; Singh *et al.*, 2018).

The analysis of the effect of catalyst dose revealed a trend in heterogeneous photocatalysis. It was observed that the degradation efficiency of Total Petroleum hydrocarbon (TPH) increase with an increasing dose of CaO nanoparticles up to an optimal point and a stable was observed. The initial increase is directly attributable to the greater availability of active sites on the nanoparticle surfaces. As more catalyst is introduced, a larger number of photons from the solar irradiation can be absorbed, generating more electron-hole pairs (e−*e*−/h+*h*+). These charge carriers are the primary agents for producing reactive oxygen species (ROS) like hydroxyl radicals (•OH) and superoxide anions ($\bullet O_2^-$), which are responsible for the oxidative breakdown of complex hydrocarbon chains into simpler, less harmful molecules like CO_2 and H_2O. However, beyond the optimal dose, the suspension becomes turbid, scattering and shielding the light from penetrating the solution, thereby reducing the photo-activation of a significant portion of the

catalyst. This phenomenon of "light shielding" is a common limitation and has been observed in other studies, including that of Saien and Nejati (2007), who reported an optimal TiO_2 concentration of 100 mg L^{-1} for refinery wastewater treatment. Furthermore, high catalyst loadings can promote agglomeration, as hinted at in the DLS data, which reduces the effective surface area and accessibility of active sites.

The effect of solution pH was found to be a vital factor, with the highest photo-catalytic efficiency in the acidic pH range. This can be rationalized by considering the surface charge of the CaO nanoparticles, which is governed by its point of zero charge (PZC). For most metal oxides, including Calcium-based nanoparticles, the surface is positively charged at a pH below the PZC. Since petroleum wastewater are predominantly non-polar or weakly polar, an acidic environment (pH < PZC) creates a more favourable condition for the adsorption of these organic molecules onto the positively charged catalyst surface through electrostatic interactions. The effective transfer of photo-generated holes and ROS to the pollutant, which results in increased deterioration, depends on this close contact. On the other hand, the catalyst surface becomes negatively charged at neutral or basic pH, which may result in an electrostatic repulsion that prevents oil components from adhering and slows down the pace of breakdown. This result is consistent with the work of Saien and Nejati (2007), who used TiO_2 to remove the most chemical Oxyen demand (COD) from wastewater from petroleum refineries at pH 3 and attributed this to the catalyst's surface charge characteristics.

A positive correlation between reaction temperature and degradation rate is expected within a moderate range. The effect of temperature on the photo-catalytic process showed a positive correlation with degradation rate within a moderate range. Increased temperature enhances molecular kinetic energy, leading to more frequent collisions between pollutants and active sites, improved mass transfer, and facilitated desorption of degradation products. However, excessively high temperatures can accelerate the recombination of electron-hole pairs, competing with the redox reactions and reducing overall photo-catalytic efficiency. The observed result agrees with conventional photo-catalytic behaviour, where an optimal temperature balances enhanced reaction kinetics with minimized charge carrier recombination. This complex interplay explains why an optimal temperature is often observed, as noted in the literature where a

temperature of 318 K (45℃) was found to be optimal for TiO_2, balancing enhanced kinetics with the mitigation of charge carrier recombination.

The effect of initial pollutant concentration demonstrated that degradation efficiency decreases as the concentration of petroleum wastewater increases. At lower concentrations (e.g., 200-400 ppm), the ratio of catalyst active sites to hydrocarbon molecules is high, allowing for efficient degradation under a fixed light intensity and catalyst dose. However, at higher concentrations (e.g., 800-1000 ppm), the fixed number of active sites and the constant flux of photons become insufficient to degrade the large quantity of pollutant molecules. Furthermore, high turbidity caused by the oil itself can limit light penetration, reducing the photon availability for exciting the catalyst. This inverse relationship between initial concentration and removal efficiency is a common feature in photo-catalytic systems.

With longer irradiation times, contact time demonstrated a steady rise in TPH degradation. The degradation efficiency improved with increased contact time, as longer irradiation durations allow for sustained photon absorption and continuous generation of ROS, enabling the progressive breakdown of refractory hydrocarbon components. This time-dependent enhancement is typical in photo-catalytic processes, where degradation rates are often rapid initially and then slow as more recalcitrant compounds remain.

5.1 CONCLUSION

The green-synthesized CaO_2 nanoparticles' photo-catalytic activity depends on a number of interconnected factors. Also, the characterization results shows that the green synthesis approach successfully produced pure, crystalline, thermally stable and nano-sized CaO nanoparticles with functional groups that supports surface activity. These photo-catalytic properties mainly suggest that the nanoparticles are well-suited for photo-catalytic degradation of petroleum wastewater where high surface area, stability and active functional groups are required.

The results of this project are consistent with the larger body of research on photo-catalysis for wastewater treatment. The proven effectiveness of onion peel-stabilized CaO nanoparticles under ideal catalyst dose, pH, temperature, and contact time settings makes this green technology a very viable, sustainable, and affordable option for cleaning up petroleum wastewater contaminated water, especially in areas prone to crude oil exploration activities.

5.2 Recommendation

i. Large-scale production of CaO-NPs should be explored due to low raw material cost.

ii. Further optimization using doped CaO nanoparticles may increase efficiency. Such as combining CaO and CuCl2 nanoparticles.

iii. Application in real oil-polluted wastewater should be tested.

iv. Additional characterization using the Brunauer-Emmett-Teller (BET) Analysis and Transmission Electron Microscopy (TEM) can improve understanding of surface behaviour of the catalyst and pollutant.

REFERENCES

Ademoroti, C. M. A. (1996). *Environmental Chemistry and Toxicology*. Foludex Press Ltd., Ibadan. pp. 44-47.

Ahmed, S., Saifullah, Ahmad, M., Swami, B. L.and Ikram, S. (2016). Green synthesis of silver nanoparticles using plant extracts and their antimicrobial applications: A review. *Journal of Advanced Research***7**(1): 17–28.

Akhtar, M. S., Panwar, J. and Yun, Y. S. (2013). Biogenic synthesis of metallic nanoparticles by plant extracts. *ACS Sustainable Chemistry and Engineering***1**(6): 591–602.

Anastas, P. T. and Warner, J. C. (1998). *Green chemistry: Theory and practice*. Oxford University Press. pp.125-129.

Barabadi, H., et al. (2019). A review on green synthesis of nanoparticles using plant extracts: Future directions and applications. *Green Chemistry Letters and Reviews***12**(1): 1–19.

Benítez, V., Mollá, E., Martín-Cabrejas, M. A., Aguilera, Y., López-Andréu, F. J. and Esteban, R. M. (2011). Onion peel as a natural antioxidant source. *Food Chemistry* **127**(1): 187–193.

Bhushan, B. (2017). *Springer handbook of nanotechnology* (4th ed.). Springer. pp. 335-361.

Daniel, M. C. and Astruc, D. (2004). Gold nanoparticles: Assembly, super molecular chemistry, quantum-size-related properties, and applications. *Chemical Society Reviews* **104**(1): 293–346.

Dreyer, D. R., Park, S., Bielawski, C. W. and Ruoff, R. S. (2010). The chemistry of graphene oxide. *Chemical Society Reviews* **39**(1): 228–240.

Dreyer, D. R., Todd, A. D. and Bielawski, C. W. (2014). Harnessing the chemistry of graphene oxide. *Chemical Society Reviews* **43**(15): 5288–5301.

El-Sayed, R. and Ramadan, A. (2016). Calcium oxide nanoparticles: synthesis and applications. *Materials Science Forum* 832, 79–95.

Fujishima, A., Zhang, X. and Tryk, D. A. (2007). Heterogeneous photocatalysis: from water photolysis to applications in environmental cleanup. *International Journal of Hydrogen Energy* **32**(14): 2664-2672.

Fujishima, A., Zhang, X., and Tryk, D. A. (2008). TiO_2 photocatalysis and related surface phenomena. *Surface Science Reports* **63**, 515–582.

Gogate, P. R. and Pandit, A. B. (2011). Advanced oxidation processes for wastewater treatment. *Industrial & Engineering Chemistry Research***50**(15): 8573–8589.

González de Mejía, E. and Vidales-Unzuetsa, A. (1997). Flavonoids in onion peel and their antioxidant activity. *Journal of Agricultural and Food Chemistry* 45, 3491–3495.

Herrmann, J. M. (2010). Photocatalysis fundamentals revisited. *Catalysis Today* **53**, 115–129.

Iravani, S. (2011). Green synthesis of metal nanoparticles using plants. *Green Chemistry***13**(10): 2638–2650.

Ishak, N. M., Kamarudin, S. K. and Timmiati, S. N. (2019). Green synthesis of metal and metal oxide nanoparticles via plant extracts: an overview. *Materials Research Express* **6**(11): 112004.

Jeevanandam, J., Barhoum, A., Chan, Y. S., Dufresne, A. and Danquah, M. K. (2018). Review on nanoparticles and nanostructured materials: History, sources, properties, and applications. *Beilstein Journal of Nanotechnology***9**, 1050–1074.

Kamat, P. V. (2010). Graphene-based nanoassemblies for energy conversion. *The Journal of Physical Chemistry Letters* **1**(2): 520–527.

Kumar, V., Yadav, S. K. and Singh, S. K. (2014). Physical and chemical methods for nanoparticle synthesis. *Journal of Nanoscience* **2014**, 1–10.

Kumari, A., Yadav, S. K., and Yadav, S. C. (2010). Biodegradable polymeric nanoparticles. *Colloids and Surfaces B: Biointerfaces*, **75**, 1–18.

Moghimi, S. M., Hunter, A. C. and Murray, J. C. (2005). Nanomedicine: Current status and future prospects. *The FASEB Journal* **19**, 311–330.

Nel, A., Xia, T., Mädler, L., and Li, N. (2006). Toxic potential of materials at the nano-level. *Science* **311**, 622–627.

Pei, S. and Cheng, H. M. (2012). The reduction of graphene oxide. *Carbon* **50**(9): 3210–3228.

Roduner, E. (2006). Size matters: Why nanomaterials are different. *Chemical Society Reviews* **35**, 583–592.

Sadhukhan, S., Ghosh, T. K., Rana, D., Roy, I., Bhattacharyya, A., Sarkar, G. and Chakraborty, M. (2016). Studies on synthesis of reduced graphene oxide (rGO) via green route and its electrical property. *Materials Research Bulletin* **79**, 41–51.

Shankar, S. S., Ahmad, A. and Sastry, M. (2004). Biosynthesis of silver nanoparticles using plants. *Biotechnology Progress***19**, 1627–1631.

Singh, J., Dutta, T., Kim, K. H., Rawat, M., Samddar, P. and Kumar, P. (2018). 'Green'synthesis of metals and their oxide nanoparticles: applications for environmental remediation. *Journal of Nanobiotechnology* **16**(1): 84.

Sivaraj, R., Rahman, P. K., Rajiv, P., Salam, H. A. and Venckatesh, R. (2014). Biogenic copper oxide nanoparticles synthesis using Tabernaemontana divaricate leaf extract and its antibacterial activity against urinary tract pathogen. *SpectrochimicaActa Part A: Molecular and Biomolecular Spectroscopy* **133**, 178-181.

Sivaraj, R., Salam, H. A. and Venckatesh, R (2014). Plant extract-mediated synthesis of metal nanoparticles. *Journal of Nanobiotechnology***12**(1): 1–10.

Stankovich, S., Dikin, D. A., Dommett, G. H. B., Kohlhaas, K. M., Zimney, E. J., Stach, E. A. and Ruoff, R. S. (2007). Graphene-based composite materials. *Nature* **442**, 282–286.

Thakkar, K. N., Mhatre, S. S. and Parikh, R. Y. (2010). Biological synthesis of metallic nanoparticles. *Nanomedicine: Nanotechnology, Biology and Medicine* **6**(2): 257-262.

Thakur, S. and Karak, N. (2015). Green reduction of graphene oxide by aqueous phytoextracts. *Carbon* **94**, 224–242.

Williams, G., Seger, B. and Kamat, P. V. (2008). TiO_2–graphene nanocomposites. *ACS Nano* **2**(7): 1487–1491.

Xi, Z., Ye, Z. and Guo, H. (2012). Graphene-based photocatalysts for hydrogen generation. *International Journal of Hydrogen Energy* **37**(21): 16306–16315.

Xing, M., Zhang, J., Chen, F. and Tian, B. (2011). An economic method to prepare vacuum activated photocatalysts with high photo-activities and photosensitivities. *Chemical Communications* **47**(17): 4947-4949.

Zhang, H., Lv, X., Li, Y., Wang, Y.and Li, J. (2010). P25-graphene composite as a high performance photocatalyst. *ACS Nano* **4**(1): 380–386.

Zhu, Y., Murali, S., Cai, W., Li, X., Suk, J. W., Potts, J. R. and Ruoff, R. S. (2011). Graphene and graphene oxide: Synthesis, properties, and applications. *Advanced Materials* **22**(35): 3906–3924.